https://doi.org/10.7494/geom.2026.20.1.49

Integrating Water Indices and Cloud-Based Engine for Change Detection of Aquaculture Areas in Lampung, Indonesia

Marindah Yulia Iswari[1]*, Indarto Happy Supriyadi[2], Doni Nurdiansah[2, 3], Kasih Anggraini[4], Nurkhalis Rahili[1], Suyarso[2]

[1] National Research and Innovation Agency (BRIN), Research Center for Hydrodynamics Technology, Surabaya, Indonesia
[2] National Research and Innovation Agency (BRIN), Research Center for Oceanology, Jakarta, Indonesia
[3] Korea Institute of Ocean Science and Technology, South Korea
[4] Regional Development Planning, Research, and Innovation Agency of Lebak, Banten, Indonesia
* Corresponding author

Abstract: Population expansion and climate change have significantly affected the coastal environment in Lampung, Indonesia, mainly through the conversion of mangroves into shrimp-farming ponds. This transformation requires effective monitoring to evaluate its impacts on coastal ecosystems and local livelihoods, as shrimp farming is a major income source in East Lampung. This research improves aquaculture detection and monitoring along the eastern coast of Lampung by integrating several water indices such as the normalized difference water index (NDWI), modified NDWI (MNDWI), water ratio index (WRI), and a newly developed water index (WI), within the cloud-based Google Earth Engine (GEE) platform to capture spatial and temporal variations. Reference data were derived from the 2019 Regional Medium-Term Development Planning Document (RPJMD) and high-resolution Google Earth imagery for accuracy assessment. Results showed that WRI combined with the Otsu's thresholding method achieved the highest performance, with an overall accuracy (OA) of 93.3% and a kappa coefficient (κ) of 86.7%. Analysis from 2018 to 2022 showed a decline in aquaculture area from 8,407.35 ha to 3,415.50 ha, aligned with statistical data on shrimp production, which decreased from 24,202 t to 8,041 t. These results indicate that the method provides a rapid and effective tool for detecting aquaculture changes, enabling local authorities to strengthen coastal management for sustainable development, ecosystem protection, and livelihood support.

Keywords: water indices, cloud-based engine, GEE, aquaculture, coastal management, Lampung, Indonesia

Received: May 16, 2025; accepted: October 10, 2025

© 2026 Author(s). This is an open-access publication that can be used, distributed, and reproduced in any medium according to the Creative Commons CC-BY 4.0 License

E-mails & ORCID iDs: marindah.yulia.iswari@brin.go.id, https://orcid.org/0000-0002-8054-3464 (M.Y.I.); https://orcid.org/0000-0002-7932-0538 (I.H.S.); https://orcid.org/0000-0001-5923-6956 (D.N.); https://orcid.org/0000-0001-5666-6504 (K.A.); https://orcid.org/0009-0000-8633-2396 (N.R.); https://orcid.org/0000-0002-6145-8029 (S.)

1. Introduction

Rapid population growth and global climate change have significantly influenced coastal dynamics – particularly in Lampung, Indonesia [1]. Lampung serves as a crucial linkage between the islands of Sumatra and Java and has exhibited notable changes in land-use patterns – especially marked by the increasing conversion of mangrove-covered areas into shrimp-farming or aquaculture ponds [2]. Notably, Lampung is Indonesia's second-largest shrimp producer; however, these land conversions pose serious threats to the coastal ecosystems that sustain local communities and livelihoods [3]. This underscores the urgent need for the precise and efficient monitoring of shrimp-farming practices to better understand and manage coastal changes – particularly in the eastern region of Lampung. Conventional monitoring techniques for coastal environments (which typically depend on manual data collection) are frequently time-consuming and require a lot of effort [4]. This inefficiency underscores the necessity for innovative solutions for accurately assessing and managing coastal resources. Therefore, remote-sensing technology has emerged as a promising alternative, providing multi-temporal and multi-spectral resolutions that significantly enhance the ability to track changes over time [5]. The multi-temporal advantage of repetitively capturing images over the same area facilitates the observation of dynamic in-land use, while the multi-spectral capacity ensures heightened sensitivity to various wavelengths, allowing for a detailed analysis of land cover and changes. Water bodies are an entity in the land-use or land-cover concept, so they can be effectively detected using multi-spectral imagery.

Water indices are widely used for detecting water bodies – one of which is the normalized difference water index (NDWI). Previous studies have employed NDWI to assess various water features such as rivers, lakes, reservoirs, and ponds [6]. Alongside the advancements in methodologies, NDWI was modified to create the modified normalized difference water index (MNDWI), which possesses enhanced capabilities for distinguishing water bodies in built-up areas [7]. Along with technological advancements, the detection of water bodies has improved through the development of various indices – including the water ratio index (WRI) and the recently introduced water index (WI) [8]. Previous research in the detection of water bodies has predominantly relied on traditional methods that have utilized remote-sensing imagery, including Landsat imagery that can be downloaded from the US Geological Survey (USGS) or Sentinel imagery that is provided by the European Space Agency (ESA) [9, 10]. However, cloud-based engines (particularly, Google Earth Engine [GEE]), have recently made these data sets available for direct analysis within an integrated online environment [11]. Compared to conventional desktop-based remote-sensing analysis, GEE offers significant advantages for developing countries, including free access to massive satellite archives, high computational efficiency, and the elimination of hardware and software limitations [11, 12]. These features make GEE particularly suited for countries like Indonesia, where limited infrastructures can hinder consistent environmental monitoring and data analysis. Recent studies

have demonstrated the effectiveness of GEE in monitoring aquaculture in Southeast Asia. For instance, [13] successfully mapped land-based aquaculture from 1990 through 2020 used edge-detection methods with high accuracy, while [14] employed GEE and backscatter data from Sentinel-1 to map coastal aquaculture ponds in Vietnam (achieving an above 90% accuracy level). These studies highlight GEE's potential to not only to enhance efficiency but also facilitate the rapid detection of water bodies, thereby enabling more-timely and precise monitoring. Building upon these foundational studies, this research aims to evaluate and monitor aquaculture farms in the Lampung area through the utilization of a cloud-based engine – particularly the integration of water indices and the free available data sets that are provided by GEE.

2. Study Area

The study area was situated along the coastal regions of East Lampung within the coordinates of 105°45′00″S–105°50′00″S and 5°22′00″E–5°43′00″E (Fig. 1).

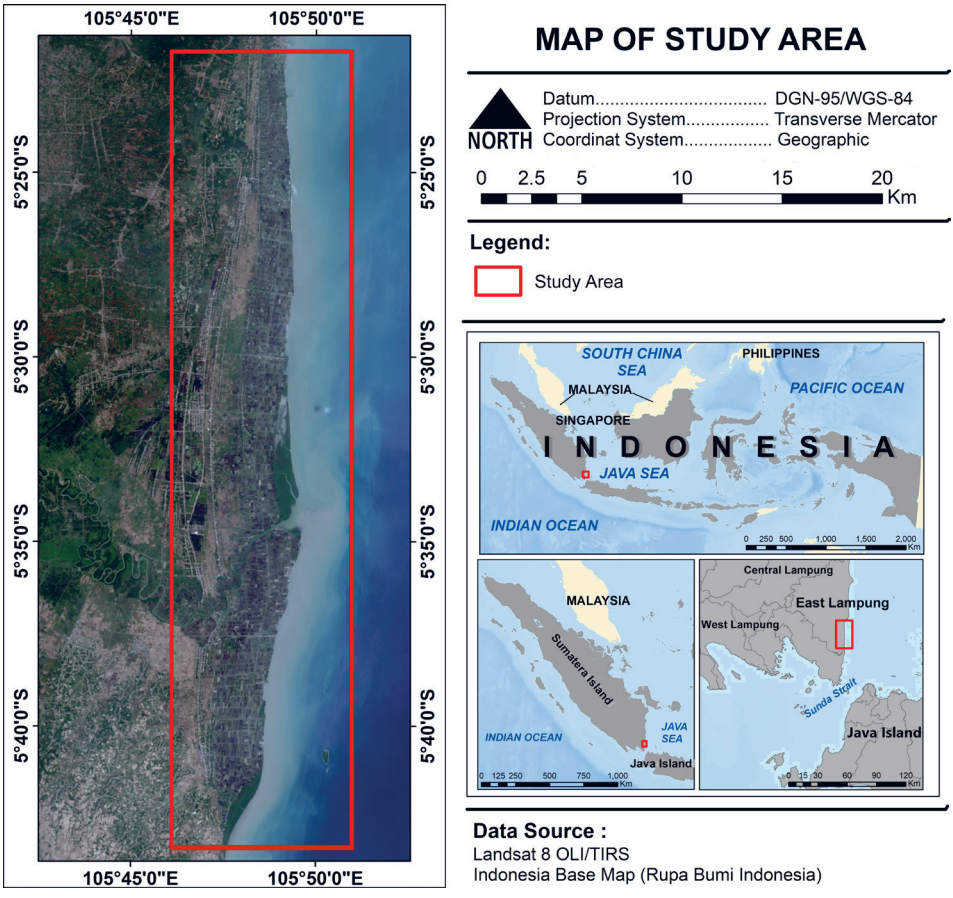

Fig. 1. Map of study area

The terrain was largely flat, with land use primarily consisting of agricultural fields, residential zones, and aquaculture sites. In East Lampung, aquaculture practices typically range from semi-intensive to intensive systems. The industry mainly focuses on shrimp farming, with numerous ponds that have been specifically designed for this purpose playing a significant role in the local economy. In the East Coast villages, shrimp aquaculture is a vital livelihood; it is not only limited to backyard hatchery businesses, but it also includes activities such as motorcycle rentals for transporting shrimp inputs to ponds, daily labor for pond preparation between culture cycles, ice production/sales, and shrimp collection [3].

3. Data and Method

3.1. Data

The imagery data that was used in this study was collected from Landsat-8 with the Onboard Operational Land Imager (OLI) sensor and the Thermal Infrared Sensor (TIRS) that was provided by the GEE data sets. Landsat-8 is an Earth observation satellite that provides publicly accessible imagery data that can be used for a variety of research applications [4].

Table 1. Landsat-8 imagery specification

Sensor	Landsat-8 OLI/TIRS
Bands	Band 1 (0.435–0.451 μm) 30 m – coastal aerosol Band 2 (0.452–0.512 μm) 30 m – blue Band 3 (0.533–0.590 μm) 30 m – green Band 4 (0.636–0.673 μm) 30 m – red Band 5 (0.851–0.879 μm) 30 m – near infrared Band 6 (1.566–1.651 μm) 30 m – shortwave infrared 1 Band 7 (2.107–2.294 μm) 30 m – shortwave infrared 2 Band 8 (0.503–0.676 μm) 15 m – panchromatic Band 9 (1.363–1.384 μm) 30 m – cirrus Band 10 (10.60–11.19 μm) 100 m – thermal infrared 1 Band 11 (11.50–12.51 μm) 100 m – thermal infrared 2
Spatial resolution	15, 30, 100 m
Temporal resolution	16 days
Data used in this study	2018 (2018-01-01 through 2018-12-31) 2019 (2019-01-01 through 2019-12-31) 2020 (2020-01-01 through 2020-12-31) 2021 (2021-01-01 through 2021-12-31) 2022 (2022-01-01 through 2022-12-31)

The advantages of Landsat-8 imagery lie in its radiometric, temporal, and spatial resolutions. Landsat-8 imagery has bands in the visible wavelength range that can be utilized for detecting water bodies. Landsat-8 imagery has a spatial resolution of 15 m for the panchromatic band, 30 m for the visible bands, and 100 m for

the thermal bands; it also has a temporal resolution of 16 days. Another advantage is that Landsat-8 imagery products are accessible for free through the United States Geological Survey (USGS) or the cloud platform that is provided by Google. Moreover, the data set from GEE has the advantage of being able to be temporally mosaicked, thereby minimizing cloud cover [15].

In this study, the Landsat-8 imagery that was used was not a single image from a single acquisition; rather, the mosaic data by GEE was compiled for an entire year of acquisition, utilizing the visible and infrared bands at a spatial resolution of 30 m. Detailed information regarding Landsat-8 imagery is presented in Table 1.

The reference data for this study was based on the Regional Medium-term Development Planning Document (RPJMD) of Lampung Province for the year 2019, which was provided by the National Geospatial Information Agency (BIG). Additionally, data was obtained from the Central Statistics Agency (BPS) for 2018, 2019, 2020, 2021, and 2022 in order to facilitate a comparison with the total aquaculture production.

3.2. Water Indices

To identify and detect water bodies, this study used four water indices; namely, NDWI, MNDWI, WRI, and WI [5, 16]. Proposed by McFeeters [17], NDWI serves as an index for extracting water bodies by integrating the spectral reflectance from the green (ρ_G) and near-infrared (ρ_{NIR}) bands. The resulting values range from –1 to 1, where positive values indicate the presence of water bodies. The calculation of NDWI can be observed in Equation (1):

$$\mathrm{NDWI} = \frac{\rho_G - \rho_{NIR}}{\rho_G + \rho_{NIR}} \tag{1}$$

As for its development, NDWI was modified by Xu [18]; this resulted in and index called MNDWI. MNDWI employs the spectral reflectance of the green (ρ_G) and short-wave infrared (ρ_{SWIR}) bands for water-body extraction and had a range from –1 to 1, where values that are greater than 0 signify the presence of water. The algorithm for MNDWI can be seen in Equation (2):

$$\mathrm{MNDWI} = \frac{\rho_G - \rho_{SWIR}}{\rho_G + \rho_{SWIR}} \tag{2}$$

WRI represents an advancement in the detection of water bodies by utilizing the reflectance from the green (ρ_G), red (ρ_R), NIR (ρ_{NIR}), and SWIR (ρ_{SWIR}) bands; this is shown in Equation (3). Water bodies are identified when the WRI value is greater than 1 [19]:

$$\mathrm{WRI} = \frac{\rho_G + \rho_R}{\rho_{NIR} + \rho_{SWIR}} \tag{3}$$

Moreover, WI is an improved version of the water body index; it utilizes reflectance that is derived from the green (ρ_G), red (ρ_R), near-infrared (ρ_{NIR}), shortwave infrared (ρ_{SWIR1}), and middle infrared (ρ_{SWIR2}) bands from Landsat TM [20]. Since the imagery that was employed in this study was from Landsat-8 OLI; however, the middle infrared band (2.08–2.35 μm) was substituted with Shortwave Infrared Band 2 (2.107–2.294 μm) due to their nearly identical wavelengths. Equation (4) illustrates the calculation of WI, where values that are greater than 0 indicate the presence of water bodies:

$$WI = 1.7204 + 171\rho_G + 3\rho_R - 70\rho_{NIR} - 45\rho_{SWIR1} - 71\rho_{SWIR2} \quad (4)$$

In this study, the thresholds that were used were the default thresholds that were determined by each water index for extracting water bodies. In the majority of the water indices, the established threshold was 0; however, there were some thresholds that also applied a value of 1 as the boundary for identifying water bodies [16]. Additionally, this research applied Otsu's threshold as a comparison to the default threshold, which is well-known for its effectiveness in establishing boundaries for identifying water bodies [22]. Otsu's threshold utilizes the maximum between-class variance criterion to determine the optimal threshold t^* for NDWI-image segmentation; its calculations are detailed in Equations (5), (6), and (7):

$$\sigma^2 = P_{nw} \cdot (M_{nw} - M)^2 + P_w \cdot (M_w - M)^2 \quad (5)$$

$$M = P_{nw} \cdot M_{nw} + P_w \cdot M_w \quad (6)$$

$$t^* = \underset{a \le t \le b}{\operatorname{Arg\,max}} \left\{ P_{nw} \cdot (M_{nw} - M)^2 + P_w \cdot (M_w - M)^2 \right\} \quad (7)$$

To reduce the bias in detecting farms, other bodies of water such as rivers and seas were excluded by using a masking method. This allowed for a more focused analysis of those areas that were specifically used for farms, thereby enhancing the accuracy of the detection algorithms.

3.3. Validation

The validation was carried by the confusion matrix method; this approach is a widely recognized technique for validating data for extracting water bodies [21]. The reference data was obtained from BIG, with random sampling conducted at various shrimp farm locations to serve as validation samples. A total of 300 sampling points were collected, encompassing both farm and non-farm sample points.

In the confusion matrix, the overall accuracy (OA) value was computed as the percentage of the correctness of the tested water indices [21]. Concurrently, the calculation of the kappa index (κ) was performed to assess the degree of the reliability

of the classifications [5]. The calculations for OA and κ can be observed in the Equation (8) and (9):

$$OA = \frac{TP + TN}{T} \tag{8}$$

$$\kappa = \frac{2 \cdot (TP \cdot TN - FN \cdot FP)}{(TP + FP) \cdot (FP + TN) + (TP + FN) \cdot (FN + TN)} \tag{9}$$

where T represents the total number of pixels in an image, TP (true positive) refers to the count of the water pixels that were accurately classified, TN (true negative) denotes the count of the non-water pixels that were accurately misclassified, FP (false positive) is the count of the pixels that were incorrectly identified as water, and FN (false negative) is the count of the water pixels that were missed [21].

The data processing was conducted through a cloud-based computational framework that leveraged GEE technology. The research workflow can be observed in the illustration that is presented in Figure 2.

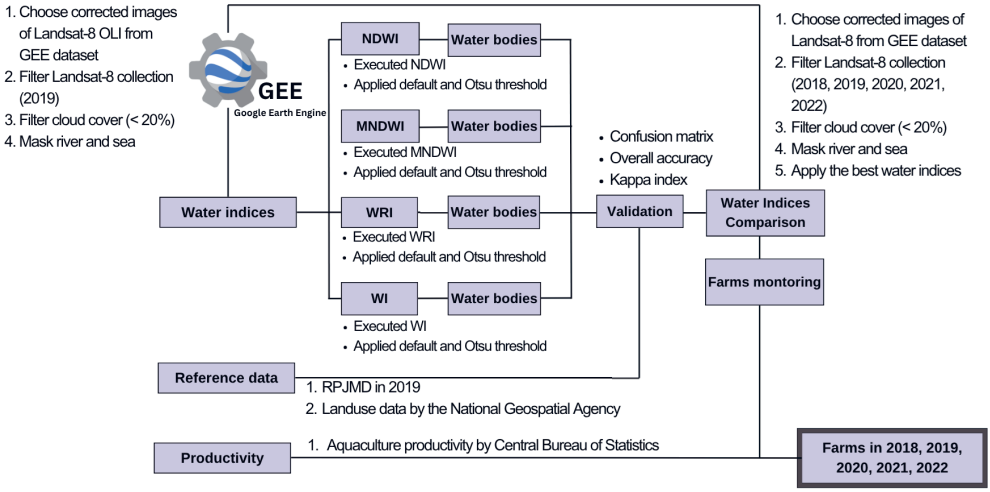

Fig. 2. Research flows

4. Results and Discussion

4.1. Water-Body Extraction

Thresholds served as delimiters between water objects and other features in the water-body extraction. This study utilized two threshold types: a default threshold, and the Otsu's threshold. The default threshold for NDWI, MDWI, and WI each

separated water bodies from other objects at a threshold of 0, with water bodies being detected at values above 0. In contrast, WRI defined water bodies as those with values above 1. Unlike the Otsu's threshold, which determines the threshold based on the values of each analyzed image, the Otsu's method computes the threshold by partitioning image pixels into foreground and background pixels in such a way that minimizes intra-class variance (or maximizes inter-class variance), resulting in indices that may vary across different images and indices [31].

Figure 3 illustrates a visual representation of the differences between using a default threshold and Otsu's threshold in detecting aquaculture through water indices. Almost all of the results from the extraction of water indices using Landsat-8 imagery from 2019 with Otsu's threshold produced representations that closely aligned with the existing conditions of the ponds in 2019. Nonetheless, some water indices captured other objects and misinterpreted them as water bodies (as demonstrated in Figure 3g); this illustrated the extraction results from MNDWI using Otsu's threshold. Furthermore, a comparison of the estimated farm areas with water indices and the area of aquaculture areas that was obtained from RPJMD 2019 can be observed in Table 2.

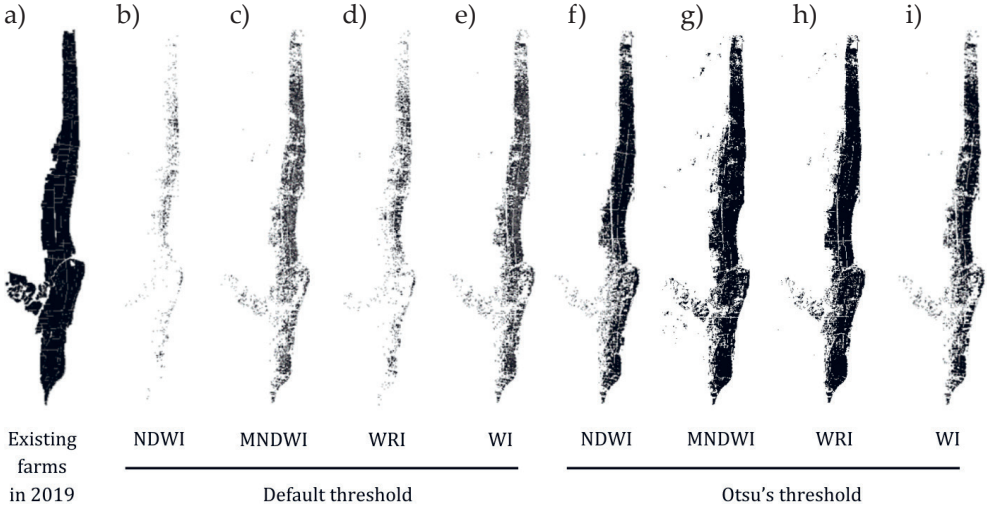

Fig. 3. Comparison of existing farms and water-body extraction based on water indices from Landsat-8 imagery in 2019

With both the visual representations and the calculation data, the deployment of Otsu's threshold yielded values that were closer to the reference data from RPJMD. Using the Otsu's threshold method, MNDWI and WRI produced area estimates that aligned closely with the RPJMD data and were linear with the visual representations. In contrast, NDWI with the default threshold resulted in a substantially underestimated area when compared with the RPJMD data.

Table 2. Comparison of farm-area estimates with water indices [ha] for 2019 and RPJMD data water indices from 2019

Water Indices	Area in 2019		
	area estimation using default threshold	area estimation using Otsu's threshold	RPJMD 2019
NDWI	605.07	5,385.96	8,662.48
MNDWI	3,372.66	8,077.95	
WRI	1,402.65	7,530.12	
WI	3,901.14	4,058.19	

4.2. Overall Accuracy and Kappa Coefficient

The reference data that was used was land-use data that was published by BIG with metadata from 2019 for the purposes of the RPJMD of Lampung Province. A total of 150 sampling sites for farms were randomly selected. To reduce the bias, an equivalent number of non-farm sampling points were also created [5], resulting in a total of 300 sampling points that included both farm and non-farm sites. Validation was performed using the confusion matrix, resulting in values for overall accuracy (OA) and kappa index (κ). A comparison of OA and κ among NDWI, MNDWI, WRI, and WI using the standard threshold and Otsu's threshold is shown in Figure 4 and Table 3.

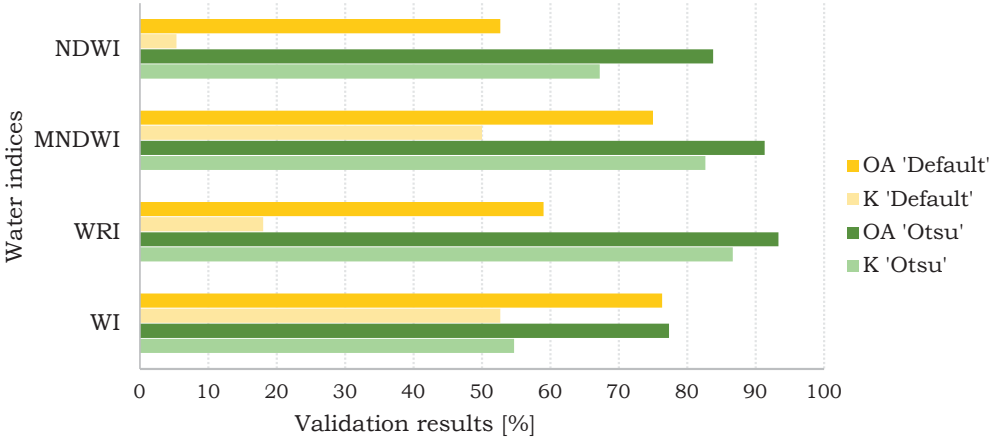

Fig. 4. Overall accuracies and kappa coefficients of NDWI, MNDWI, WRI, and WI based on reference data that was obtained from RPJMD 2019

Table 3. Validation test results for water indices from 2019 using reference data from the RPJMD 2019

Validation	NDWI	MNDWI	WRI	WI
κ 'Otsu'	0.672	0.827	0.867	0.547
OA 'Otsu'	0.838	0.913	0.933	0.773
κ 'Default'	0.053	0.500	0.180	0.527
OA 'Default'	0.527	0.750	0.590	0.763

The validation results indicated that the OA and κ values with Otsu's threshold exhibited a higher tendency compared to those that were obtained with the default threshold. This was consistent with the representation of the water indices that used Otsu's threshold, which aligned more closely with the visualization of the existing ponds in Lampung. MNDWI yielded an OA level of 0.913 and a κ coefficient of 0.827. As an enhanced methodological approach, MNDWI offered superior detail relative NDWI [23]. This increased level of detail suggests that MNDWI effectively eliminated features that could have obstructed the identifications of water bodies, including vegetation, soil, and urban development [18]. This finding aligned with previous research, which demonstrated that MNDWI achieved accuracy rates that exceeded 90% in detecting aquaculture ponds in India [23]. Additionally, MNDWI was identified as the sole index that was capable of enhancing the visibility of water surfaces and proved to be the most effective in delineating water bodies within floodplains in Hungary [24]. In the Loess Plateau region of China, MNDWI similarly delineated the boundaries of both small and large ponds [25]. However, it is important to consider the noise that may have been encountered in each study area when using MNDWI. In this study, MNDWI produced an overestimation because it detected clouds and marshes that were not part of the pond areas.

Meanwhile, WRI produced slightly higher validation values when compared to MNDWI, with OA and κ coefficient levels of 0.933 and 0.867, respectively. WRI is an index that integrates multiple spectral bands, including green, red, near infrared, and shortwave infrared [19]. Compared to MNDWI, WRI showed marginally higher accuracy based on both the OA and κ coefficient values. This finding aligned with the research of [26], which indicated that WRI effectively mapped the boundaries of aquaculture sites, mirroring ground-truth results in Uttarakhand, India. Conversely, MNDWI is recommended as the index that is suitable for enhancing urban spatial planning and managing flood-disaster control by urban planners for those areas that are subject to flooding within metropolitan zones [27]. In this study, WRI produced clearer delineations of water bodies compared to the results from MNDWI; this improved delineation coincided with the reductions in cloud and shadow noise when using WRI. This reduction in noise was not limited to water bodies but was also

observed across other land-use types, thus suggesting that clouds could be consistently mitigated by adopting WRI across different contexts [8]. Although WRI yielded the highest OA and κ levels in this study, its applicability to other coastal areas remains conditional; this is because environmental conditions and sample selection influence its validation outcomes [31]. The noise that is generated by clouds and their shadows is minimized in WRI. Furthermore, this observation is consistent with other land-use types, thus indicating that the presence of clouds can be effectively mitigated using this index [8].

To assess the performance of the individual indices in the subsequent years, the accuracy tests were interpreted visually using high-resolution Google Earth imagery. Sampling was performed through visual interpretation by year, with a total of 300 points; these were evenly divided into 150 points for farms and 150 points for non-farms. Google Earth provides multitemporal information with high resolution, albeit with limitations in its multispectral capabilities [32]. The comparison between using the reference data from Google Earth and RPJMD in 2019 revealed notable divergences in the OA and κ values (as shown in Table 4). For 2019, employing RPJMD data yielded the highest OA level (exceeding 0.9), as was indicated in the MNDWI and WRI analyses with the Otsu's threshold. In addition to achieving a high OA level, the use of the RPJMD reference data provided a level of confidence that was nearly perfect (as was indicated by a κ value that exceeded 0.81) [34]. By contrast, the calculations based on the Google Earth reference data produced a maximum OA level of 0.81 and a maximum κ level of 0.62 (as shown in the NDWI analysis with the default threshold). Therefore, the RPJMD reference data provided robust validation that maximized the OA and κ values in this study (greater than 0.90 and 0.81, respectively).

Table 4. Comparison of validation using reference data from RPJMD and Google Earth for 2019

RPJMD 2019		Default threshold	Otsu's threshold	Google Earth 2019		Default threshold	Otsu's threshold
NDWI	OA	0.527	0.838	NDWI	OA	0.593	0.810
	κ	0.053	0.672		κ	0.187	0.620
MNDWI	OA	0.750	0.913	MNDWI	OA	0.760	0.747
	κ	0.500	0.827		κ	0.520	0.493
WRI	OA	0.590	0.933	WRI	OA	0.667	0.777
	κ	0.180	0.867		κ	0.333	0.553
WI	OA	0.763	0.773	WI	OA	0.780	0.793
	κ	0.527	0.547		κ	0.560	0.587

A comparison of the OA and κ levels across all of the indices and years is shown in Table 5. The validation that used reference data from Google Earth indicated a tendency for those analyses that employed the Otsu's threshold to yield higher OA levels when compared with the analyses that used the default threshold. For example, the OA level of NDWI was 0.56 with the default threshold for 2021, while the OA level with the Otsu's threshold analysis hovered at around 0.767. Differences could also be observed in the value of κ, which tended to be below 0.8; this indicated a lower confidence level in the analysis [34]. In some calculations, however, the Google Earth reference data could produce OA levels of up to 0.910 with κ levels reaching 0.820 for WRI 2018 with the Otsu's threshold. The NDWI, MNDWI, and WI indices for that year also yielded OA levels above 0.80, thus suggesting that using Google Earth could be a viable option when ground-truth reference data such as RPJMD is unavailable.

Table 5. Comparison of OA and κ levels with sampling from Google Earth

Water Index	2018		2019		2020		2021		2022	
	OA	κ	OA	κ	OA	κ	OA	κ	OA	κ
Default										
NDWI	0.577	0.153	0.593	0.187	0.630	0.260	0.560	0.120	0.573	0.147
MNDWI	0.820	0.640	0.760	0.520	0.710	0.420	0.787	0.573	0.743	0.487
WRI	0.637	0.273	0.667	0.333	0.710	0.420	0.623	0.247	0.627	0.253
WI	0.847	0.693	0.780	0.560	0.723	0.447	0.767	0.533	0.75	0.500
Otsu										
NDWI	0.837	0.673	0.810	0.620	0.727	0.453	0.767	0.533	0.710	0.420
MNDWI	0.827	0.653	0.747	0.493	0.633	0.267	0.760	0.520	0.713	0.427
WRI	0.910	0.820	0.777	0.553	0.713	0.427	0.783	0.567	0.640	0.280
WI	0.847	0.693	0.793	0.587	0.737	0.473	0.780	0.560	0.757	0.513

4.3. Monitoring Aquaculture and Sustainable Coastal Management in Lampung

Annual area estimation calculations are required to monitor changes based on the estimates from each index. The area estimates are computed in GEE processing using both the default threshold and the Otsu's threshold for the years 2018, 2019, 2020, 2021 and 2022 on NDWI, MNDWI, WRI, and WI. Table 6 presents a comparison of the area estimates for each index in hectares.

Table 6. Estimated farm areas using water indices for years 2018, 2019, 2020, 2021, and 2022 [ha]

Year	NDWI		MNDWI		WRI		WI		RPJMD
	Default threshold	Otsu's threshold	Default threshold	Otsu's threshold	Default threshold	Otsu's threshold	Default threshold	Otsu's threshold	
2018	742.50	5,509.89	5,102.01	9,655.29	1,842.39	8,407.35	5,323.95	5,483.97	8,662.48
2019	605.07	5,385.96	3,372.66	8,077.95	1,402.65	7,530.12	3,901.14	4,058.19	
2020	1,568.90	5,328.45	7,318.08	10,203.66	2,853.90	3,941.01	6,512.40	6,657.66	
2021	1,315.20	5,982.39	6,375.24	8,613.45	2,459.07	5,773.05	5,982.39	6,118.74	
2022	1,786.40	5,445.90	6,777.99	9,782.91	3,147.12	3,415.50	6,330.42	6,453.81	

It was evident that, in all of the years, the area estimates were underestimates when using the default threshold. This was particularly notable for the NDWI index, which yielded estimates that were lower than the overall average when compared with the other indices (with a value of 742.50 ha). By contrast, the data that was most reliable for comparison was the 2019 data that referenced RPJMD; here, the calculations that used the Otsu's threshold more closely approximated the reference area than those that used the default threshold. In several studies on surface water monitoring, the Otsu's threshold produced high accuracy, with overall accuracy (OA) values exceeding 90% [32, 33]. Therefore, the Otsu's threshold in this study aligned with the findings from previous research.

To examine the relationship between the estimated farm area and productivity, this study utilized productivity data from BPS. The area estimates that were compared were those that were derived from the index analysis with the highest validation. Between 2018 and 2022, the data analysis revealed a general decline in area of aquaculture; a notable exception was 2021, when an increase could be observed (Fig. 5). Similarly, the data from BPS indicated a downward trend in aquaculture productivity (measured in tons) over the same period. This parallel decline suggested a consistent trend between the reducing aquaculture area and the overall productivity in East Lampung during these years.

Estimation area diagrams that used water indices showed a declining trend from 2018 to 2020, with a rise in 2021 and a subsequent decline again in 2022. Meanwhile, the productivity graph showed declines from 2018 through 2021, with a slight increase in 2022. From this analysis, a divergent trend occurred in 2021, where the estimated area increased while productivity decreased. The decline in productivity in 2021 was driven by deteriorating environmental quality that triggered disease outbreaks accompanied by environmental degradation due to coastal activity pressure, changes in land use for industry and transportation, and a shift of the cultivated land from semi-intensive/intensive ponds to traditional ponds [35]. According to

archives from the National Agency for Disaster Management (BNPB) and BPS, East Lampung additionally experienced four flood events in a year; the highest number that was recorded within the 2018–2024 period (with the greatest disaster occurring in December 2021) [36]. This condition may have contributed to the observed increase in the estimated pond area for that year.

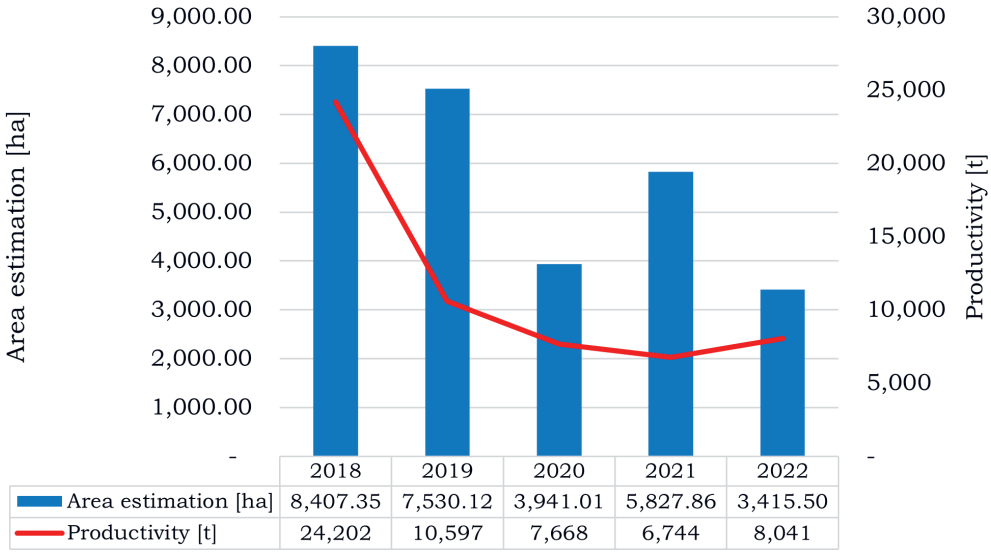

	2018	2019	2020	2021	2022
Area estimation [ha]	8,407.35	7,530.12	3,941.01	5,827.86	3,415.50
Productivity [t]	24,202	10,597	7,668	6,744	8,041

Fig. 5. Comparison of aquaculture area estimates from data analysis with productivity data from BPS

From the results of this analysis, the use of water indices in this study proved to be efficient for examining the spatial dynamics of the area (particularly, shrimp farms) over the specific temporal periods. This aligned with the prior studies that reported water indices as being effective for mapping small water bodies (especially in tropical regions); however, they were less suitable in snow-covered areas [5, 21, 28]. However, the selection of the reference data influenced the validation analysis in this study. The reference data that was derived from Google Earth yielded lower validation values for both OA and κ. In contrast, the reference data that was obtained from RPJMD (which was official data that was collected from censuses and field surveys) produced higher OA and κ values. Additionally, this method can also enable the modeling and prediction of farm areas, which can be correlated with productivity; therefore, the government should consider adopting this approach as a quick and efficient way to manage aquaculture for sustainable coastal development.

Shrimp commodity production in Lampung ranks fifth nationally in Indonesia according to the Regional Development Planning Agency of Lampung Province (Bappeda Lampung). In line with this, the local government seeks to strengthen the economy in the rural and coastal areas that are focused on aquaculture management,

marketing, and the supervision of marine and fishery resources (as outlined in the RPJMD document) [29]. This research can be adapted to support one of these initiatives – specifically managing the aquaculture sector. This includes establishing a systematic monitoring program that utilizes free cloud-data-set analysis to evaluate and track changes in farm areas over time [5], integrating productivity data to assess the potential output of shrimp farms [30], and encouraging data collection from stakeholders and farmers in order to enrich the database with real productivity data (thereby improving future assessments). However, policymakers should also develop regulations for land modifications of shrimp ponds with careful considerations of coastal ecosystems in order to promote environmental sustainability and optimal land use. Implementing these recommendations can serve as an effective approach to managing the coast smartly and efficiently, thus fostering harmony between environmental conservation and livelihoods for a sustainable coastal region – especially along the eastern coast of Lampung.

4.4. Limitations

The application of water indices can facilitate the rapid estimation of aquaculture distribution with enhanced efficiency – particularly the shrimp farms in Lampung Province. Nonetheless, this study faced limitations that were associated with the utilization of multispectral satellite imagery. The effectiveness of water indices that depend on multiple spectral channels for extracting water bodies from satellite images decreases significantly when the cloud cover exceeds 50%; consequently, this method's ability to distinguish between cloud shadows and actual water bodies was compromised, as both features can exhibit similar spectral characteristics in certain bands. This similarity may result in misclassifications and overestimations of aquaculture areas. Another limitation lay in the 30-meter spatial resolution of the Landsat-8 imagery, which posed challenges in accurately detecting small-scale aquaculture ponds; this potentially resulted in omission errors or underestimations of aquaculture areas. It is advisable to integrate multi-satellite images in future research to reduce the distortions that are caused by cloud cover. In addition, the use of annual data acquisitions that have been collected to produce cloud-free imagery has limitations for intra-annual dynamics, thereby reducing the sensitivity of monitoring short-term or seasonal variations in aquaculture activities. This limitation can be mitigated through gradual mapping from a single acquisition imagery (although this requires additional time for analysis).

5. Conclusion

This research applied water indices such as NDWI, MNDWI, WI, and WRI to identify aquaculture areas in the coastal region of East Lampung. Among these water indices, WRI that employed the Otsu's threshold method and RPJMD as the

reference data demonstrated results that extracted the aquaculture areas with the highest accuracy; this was evidenced by the overall accuracy and kappa coefficient (93.3% and 86.7%, respectively). The use of reference data with Google Earth in this study proved to be insufficient for maximizing the validation analysis, given its trend of low OA values and its low confidence with κ values. As was estimated by these water indices between 2018 and 2022, the changes in the aquaculture area exhibited a decreasing trend. This trend correlated with statistical data on shrimp farm productivity that was obtained from the national data that was provided by BPS. Therefore, the use of water indices that are derived from free cloud data sets through a cloud-based engine (particularly GEE) can be regarded as a viable approach for estimating any changes in aquaculture areas in East Lampung. This approach provides a scalable framework that can be adapted for monitoring dynamic aquaculture activities in other coastal provinces in Indonesia – particularly those that are facing challenges in sustainable coastal management. By providing insights into aquaculture dynamics, the findings support the formulation of conservation strategies and sustainable development policies. These contributions align with broader environmental management goals, thus promoting a balance between ecological integrity and economic growth in coastal communities. To further improve the accuracy, future research could explore the use of multi-temporal satellite imagery to reduce cloud-cover issues. Additionally, integrating productivity data that is obtained from farmers over specific periods may enhance the accuracy. More-detailed data integration has the potential to facilitate rapid, precise, and detailed predictions of productivity in the forthcoming period. The findings of this study can be incorporated into existing coastal zoning and aquaculture licensing systems, providing an evidence-based tool for supporting spatial planning, permit regulation, and regulatory enforcement – particularly in those regions where rapid land-use change threatens ecological sustainability.

Funding

This research is part of the COREMAP-CTI monitoring that was conducted in 2018 by the Research Center for Oceanography (formerly, the Indonesian Institute of Sciences) in Lampung.

CRediT Author Contribution

M. Y. I: conceptualization, writing – original draft, writing – review & editing, methodology, formal analysis and validation.

I. H. S: data curation, investigation, writing – review & editing.

D. N: data curation, formal analysis.

K. A: data curation, visualization.

N. R: formal analysis, writing – review & editing.

S: supervision, writing – review & editing.

Declaration of Competing Interests

The authors declare that they have no known competing financial interests nor personal relationships that could have appeared to influence the work that was reported in this paper.

Data Availability

The public data in this article include:

- Landsat-8 Imagery available at https://developers.google.com/earth-engine/datasets/catalog/landsat-8;
- Regional Development Planning Document 2019–2024 available at https://ppid.lampungprov.go.id/page/RPJMD-Provinsi-Lampung-Tahun-2019-2024;
- Aquaculture Production of Lampung available at https://lampung.bps.go.id/.

Use of Generative AI and AI-Assisted Technologies

Generative AI tools were used only for translation and language editing. No AI tools were used for data analysis, interpretation, conceptual development, visualization or drawing scientific conclusions.

Acknowledgements

The authors would like to thank Doni Widyasmoro from the Office of Marine and Fisheries of Lampung (DKP Lampung) for assisting with the field survey. The authors also thank the National Geospatial Agency (BIG) for providing the reference data as well as the GEE community for sharing useful sample codes and data sets. Additionally, the authors express their gratitude to the Research Center for Oceanography (PRO), the Research Center for Hydrodynamics Technology (PRTH), and the National Research and Innovation Agency (BRIN).

References

[1] Tarigan T.A., Nurisman N., Simarmata N.: *Identification of coastal problem along the east coast of Lampung, Indonesia*, [in:] *Proceedings of the 7th International Seminar on Ocean and Coastal Engineering. Environmental and Natural Disaster Management (ISOCEEN 2019)*, SciTePress – Science and Technology Publications, Setúbal 2021, pp. 138–142.

[2] Bakri S., Hartati F., Kaskoyo H., Febriyano I.G., Dewi B.S.: *The fate of mangrove ecosystem sustainability on the shrimp cultivation area in Tulang Bawang District, Lampung, Indonesia*. Biodiversitas Journal of Biological Diversity, vol. 24(1), 2023, pp. 379–390. https://doi.org/10.13057/BIODIV/D240145.

[3] Tobey J., Poespitasari J.H., Wiryawan B.: *Good practices for community-based planning and management of shrimp aquaculture in Sumatra, Indonesia*. World Bank, NACA, WWF and FAO Consortium Program on Shrimp Farming and the Environment, 2000.

[4] Masria A.: *Bridging coastal challenges: The role of remote sensing and future research*. Regional Studies in Marine Science, vol. 73, 2024, 103502. https://doi.org/10.1016/j.rsma.2024.103502.

[5] Tew Y.L., Sabjan A., Lee L.K., See K.F., Wee S.T.: *Comparison of three water indices for tropical aquaculture ponds extraction using Google Earth Engine*. Sains Malaysiana, vol. 51(2), 2022, pp. 369–378. http://doi.org/10.17576/jsm-2022-5102-04.

[6] Subedi A., Acharya T.D.: *Small water bodies detection and evaluation using normalized difference water index (NDWI) from Landsat image in Western Terai, Nepal*. Bulletin of Nepal Hydrogeological Association, vol. 6, 2021, pp. 89–96.

[7] Albertini C., Gioia A., Iacobellis V., Manfreda S.: *Detection of surface water and floods with multispectral satellites*. Remote Sensing, vol. 14(23), 2022, 6005. https://doi.org/10.3390/rs14236005.

[8] Liu S., Wu Y., Zhang G., Lin N., Liu Z.: *Comparing water indices for Landsat data for automated surface water body extraction under complex ground background: A case study in Jilin Province*. Remote Sensing, vol. 15(6), 2023, 1678. https://doi.org/10.3390/rs15061678.

[9] Kwang C., Jnr E.M.O., Amoah A.S.: *Comparing of Landsat-8 and Sentinel 2A using water extraction indexes over Volta River*. Journal of Geography and Geology, vol. 10(1), 2017, pp. 1–7. https://doi.org/10.5539/jgg.v10n1p1.

[10] Bhaga T.D., Dube T., Shekede M.D., Shoko C.: *Investigating the effectiveness of Landsat-8 OLI and Sentinel-2 MSI satellite data in monitoring the effects of drought on surface water resources in the Western Cape Province, South Africa*. Remote Sensing Applications: Society and Environment, vol. 32, 2023, 101037. https://doi.org/10.1016/j.rsase.2023.101037.

[11] Amani M., Ghorbanian A., Ahmadi S.A., Kakooei M., Moghimi A., Mirmazloumi S.M., Moghaddam S.H.A., Mahdavi S., Ghahremanloo M., Parsian S., Wu Q., Brisco B.: *Google Earth Engine cloud computing platform for remote sensing big data applications: A comprehensive review*. IEEE Journal of Selected Topics in Applied Earth Observations and Remote Sensing, vol. 13, 2020, pp. 5326–5350. https://doi.org/10.1109/JSTARS.2020.3021052.

[12] Tamiminia H., Salehi B., Mahdianpari M., Quackenbush L., Adeli S., Brisco B.: *Google Earth Engine for geo-big data applications: A meta-analysis and systematic review*. ISPRS Journal of Photogrammetry and Remote Sensing, vol. 164, 2020, pp. 152–170. https://doi.org/10.1016/j.isprsjprs.2020.04.001.

[13] Zhang C., Cui Y., Xie H.: *Mapping of land-based aquaculture regions in Southeast Asia and its spatiotemporal change from 1990 to 2020 using time-series remote sensing data*. International Journal of Applied Earth Observation and Geoinformation, vol. 121, 2023, 103432. https://doi.org/10.1016/j.jag.2023.103432.

[14] Sun Z., Luo J., Yang J., Yu Q., Zhang L., Xue K., Lu L.: *Nation-scale mapping of coastal aquaculture ponds with Sentinel-1 SAR data using Google Earth Engine*. Remote Sensing, vol. 12(18), 2020, 3086. https://doi.org/10.3390/rs12183086.

[15] Soulard C.E., Walker J.J., Petrakis R.E.: *Implementation of a surface water extent model in Cambodia using cloud-based remote sensing*. Remote Sensing, vol. 12(6), 2020, 984. https://doi.org/10.3390/rs12060984.

[16] Yu Z., Di L., Rahman M.S., Tang J.: *Fishpond mapping by spectral and spatial-based filtering on Google Earth Engine: A case study in Singra Upazila of Bangladesh*. Remote Sensing, vol. 12(17), 2020, 2692. https://doi.org/10.3390/rs12172692.

[17] McFeeters S.K.: *The use of the normalized difference water index (NDWI) in the delineation of open water features*. International Journal of Remote Sensing, vol. 17(7), 1996, pp. 1425–1432. https://doi.org/10.1080/01431169608948714.

[18] Xu H.: *Modification of normalised difference water index (NDWI) to enhance open water features in remotely sensed imagery*. International Journal of Remote Sensing, vol. 27(14), 2006, pp. 3025–3033. https://doi.org/10.1080/01431160600589179.

[19] Shen L., Li C.: *Water body extraction from Landsat ETM+ imagery using AdaBoost algorithm*, [in:] *2010 18th International Conference on Geoinformatics*, IEEE, 2010, pp. 1–4. https://doi.org/10.1109/GEOINFORMATICS.2010.5567762.

[20] Fisher A., Flood N., Danaher T.: *Comparing Landsat water index methods for automated water classification in eastern Australia*. Remote Sensing of Environment, vol. 175, 2016, pp. 167–182. https://doi.org/10.1016/j.rse.2015.12.055.

[21] Acharya T.D., Subedi A., Lee D.H.: *Evaluation of water indices for surface water extraction in a Landsat-8 scene of Nepal*. Sensors, vol. 18(8), 2018, 2580. https://doi.org/10.3390/s18082580.

[22] Xu X., Xu S., Jin L., Song E.: *Characteristic analysis of Otsu threshold and its applications*. Pattern Recognition Letters, vol. 32(7), 2011, pp. 956–961. https://doi.org/10.1016/j.patrec.2011.01.021.

[23] Rani P.P., Kumar M.S., Sireesha P.G.: *Mapping of active and empty aquaponds using spectral indices in coastal region of Guntur District, Andhra Pradesh, India*. Journal of Environmental Biology, vol. 42(5), 2021, pp. 1338–1346. http://doi.org/10.22438/jeb/42/5/MRN-1634.

[24] Szabo S., Gácsi Z., Balazs B.: *Specific features of NDVI, NDWI and MNDWI as reflected in land cover categories*. Landscape & Environment, vol. 10(3–4), 2016, pp. 194–202. https://doi.org/10.21120/LE/10/3-4/13.

[25] Guo J., Wang X., Liu B., Liu K., Zhang Y., Wang C.: *Remote-sensing extraction of small water bodies on the Loess Plateau*. Water, vol. 15(5), 2023, 866. https://doi.org/10.3390/w15050866.

[26] Deoli V., Kumar D., Kumar M., Kuriqi A., Elbeltagi A.: *Water spread mapping of multiple lakes using remote sensing and satellite data*. Arabian Journal of Geosciences, vol. 14, 2021, pp. 1–15. https://doi.org/10.1007/s12517-021-08597-9.

[27] Mukherjee N.R., Samuel C.: *Assessment of the temporal variations of surface water bodies in and around Chennai using Landsat imagery*. Indian Journal of Science and Technology, vol. 9(18), 2016, pp. 1–7. https://doi.org/10.17485/ijst/2016/v9i18/92089.

[28] Rahaman M.H., Masroor M., Sajjad H.: *Integrating remote sensing derived indices and machine learning algorithms for precise extraction of small surface water bodies in the lower Thoubal River watershed, India*. Journal of Cleaner Production, vol. 422, 2023, 138563. https://doi.org/10.1016/j.jclepro.2023.138563.

[29] Bappeda Lampung: *Rencana Pembangunan Jangka Menengah Daerah (RPJMD) Provinsi Lampung 2019–2024* [Regional Development Planning Document]. 2019. https://ppid.lampungprov.go.id/page/RPJMD-Provinsi-Lampung-Tahun-2019-2024 [access: August 9, 2025].

[30] Peng Y., Sengupta D., Duan Y., Chen C., Tian B.: *Accurate mapping of Chinese coastal aquaculture ponds using biophysical parameters based on Sentinel-2 time series images*. Marine Pollution Bulletin, vol. 181, 2022, 113901. https://doi.org/10.1016/j.marpolbul.2022.113901.

[31] Kirchner J.W., Hooper R.P., Kendall C., Neal C., Leavesley G.: *Testing and validating environmental models*. Science of The Total Environment, vol. 183(1–2), 1996, pp. 33–47. https://doi.org/10.1016/0048-9697(95)04971-1.

[32] Li W., Dong R., Fu H., Wang J., Yu L., Gong P.: *Integrating Google Earth imagery with Landsat data to improve 30-m resolution land cover mapping*. Remote Sensing of Environment, vol. 237, 2020, 111563. https://doi.org/10.1016/j.rse.2019.111563.

[33] Rad A.M., Kreitler J., Sadegh M.: *Augmented Normalized Difference Water Index for improved surface water monitoring*. Environmental Modelling & Software, vol. 140, 2021, 105030. https://doi.org/10.1016/j.envsoft.2021.105030.

[34] Landis J.R.. Koch G.G.: *The measurement of observer agreement for categorial data*. Biometrics, vol. 33(1), 1977, pp. 159–174. https://doi.org/10.2307/2529310.

[35] Utama D., Widigdo B., Kamal M.M., Taryono T.: *Site suitability evaluation of Whiteleg shrimp ponds operated using different farming systems in the coastal of East Lampung Regency, Indonesia*. Jurnal Riset Akuakultur, vol. 17(4), 2023, pp. 235–248. https://doi.org/10.15578/jra.17.4.2022.235-248.

[36] Muhari A.: *Curah hujan tinggi, 150 KK terdampak banjir di Kabupaten Lampung Timur* [Heavy rainfall affects 150 families in East Lampung Regency]. BNPB (Badan Nasional Penanggulangan Bencana), December 31, 2021. https://www.bnpb.go.id/berita/curah-hujan-tinggi-150-kk-terdampak-banjir-di-kabupaten-lampung-timur [access: August 9, 2025].